Amino Acids (2025) 57:37
https://doi.org/10.1007/s00726-025-03464-3

ORIGINAL ARTICLE

CacyBP/SIP - RPL6 interaction: potential influence on ribosome function

Ewelina Jurewicz[1] · Małgorzata Maksymowicz-Trivedi[1] · Omid Saberi-Khomami[1] · Olga Iwańska[2] · Agata Starosta[2] · Ewa Kilańczyk[1] · Paweł Bieganowski[4] · Adam Jarmuła[1] · Wiesława Leśniak[1] · Sławomir Filipek[3] · Anna Filipek[1]

Received: 30 April 2025 / Accepted: 10 June 2025

Abstract

Previously, we have shown that CacyBP/SIP interacts with NPM1, a protein involved in ribosome biogenesis. In this work, we extended our previous studies to look for the potential impact of CacyBP/SIP on ribosome biogenesis and/or function. Using mass spectrometry analysis, we have found that several RPs could be potential CacyBP/SIP targets. Since RPL6 was one of the proteins with the best quality scores identified in this analysis we focused on the possible interaction between CacyBP/SIP and RPL6. By applying various biochemical methods, we confirmed this interaction and showed that it was direct. Moreover, in silico analysis allowed us to establish the domains/fragments of both proteins involved in the binding. To further explore the possible role of CacyBP/SIP in ribosome function we performed several analyses using neuroblastoma NB2a cell line with stably silenced CacyBP/SIP expression. We have found, by applying OPP (O-propargyl-puromycin), which labels nascent polypeptides, that the number of cells with enhanced staining in the perinuclear area, reminiscent of rough ER localization, was significantly lower in the cell line with diminished CacyBP/SIP level. To verify the influence of CacyBP/SIP on the efficiency of protein synthesis we investigated the level of Hsp70, a stress-inducible protein, in NB2a cells subjected to heat shock. The results, showing markedly higher Hsp70 production in control cells, indicate that CacyBP/SIP, most probably through interaction with RPL6 and/or other RPs, may have some influence on ribosome function and, possibly, on protein synthesis in the cell.

Keywords CacyBP/SIP · Molecular modeling · Protein synthesis · Ribosome · RPL6

Abbreviations

CacyBP/SIP	Calcyclin binding protein/Siah-1 interacting protein
EMEM	Eagle's Minimum Essential Medium
FBS	Fetal bovine serum
Hsp70	70 kDa heat shock protein
IP	Immunoprecipitation
IPTG	isopropyl β- d-1-thiogalactopyranoside
LB	Lysogeny broth
MD	Molecular dynamic
NPM1	Nucleophosmin 1 or nucleolar phosphoprotein B23 or numatrin
OPP	O-propargyl-puromycin
PBS-T	Phosphate buffered saline containing Tween 20
PLA	Proximity ligation assay
RPL6	Ribosomal protein L6
RPs	Ribosomal proteins
RT-qPCR	Real time-quantitative PCR

Ewelina Jurewicz and Małgorzata Maksymowicz-Trivedi have contributed equally to this work.

Communicated by R. Dave

✉ Sławomir Filipek
sh.filipek@uw.edu.pl

✉ Anna Filipek
a.filipek@nencki.edu.pl

[1] Nencki Institute of Experimental Biology, Polish Academy of Sciences, 3 Pasteur Street, Warsaw 02-093, Poland

[2] Institute of Biochemistry and Biophysics, Polish Academy of Sciences, 5a Pawińskiego Street, Warsaw 02-106, Poland

[3] Faculty of Chemistry, Biological and Chemical Research Centre, University of Warsaw, 1 Pasteur Street, Warsaw 02-093, Poland

[4] Mossakowski Medical Research Institute, Polish Academy of Sciences, 5 Pawińskiego Street, Warsaw 02-106, Poland

Published online: 22 July 2025

TBS Tris buffered saline

Introduction

The CacyBP/SIP protein was originally discovered as an S100A6 (calcyclin) ligand (Filipek and Wojda 1996; Filipek and Kuznicki, 1998) and later found to be a Siah-1 binding partner (Matsuzawa and Reed 2001). CacyBP/SIP is expressed in different mammalian cells and tissues, including brain where it is present mainly in neurons (Jastrzębska et al., 2000). Studies on neuroblastoma cell lines, NB2a and SH-SY5Y, have shown that CacyBP/SIP is mainly a cytosolic protein although, to a lesser extent, it is also present in the cell nucleus (Rosińska and Filipek 2018).

CacyBP/SIP is a multi-ligand and multifunctional protein. It binds some members of the S100 protein family, components of E3 ubiquitin ligase, such as Siah-1 and Skp1, cytoskeletal proteins including tubulin, actin and tropomyosin, MAP kinases such as ERK1/2 and p38, heat shock protein Hsp90 and nuclear protein NPM1 (Topolska-Woś et al. 2016; Filipek and Leśniak 2018). As to the E3 ligase, it has been suggested that the major role of CacyBP/SIP is to stabilize the association of its various components and orchestrate the correct distance and orientation of the ligase towards β-catenin (Matsuzawa and Reed 2001; Liu et al. 2001; Dimitrova et al. 2010). Through interaction with tubulin, actin and tropomyosin CacyBP/SIP seems to be involved in cell proliferation, differentiation and, in consequence, in development, aging and neurodegeneration (Schneider et al. 2007, 2010; Jurewicz et al. 2013). Studies of the CacyBP/SIP role in cell proliferation, mainly in development of different tumors, have shown upregulation of CacyBP/SIP level in pancreatic, gastric and colon cancer, nasopharyngeal carcinoma, osteogenic sarcoma, melanoma, and breast cancer (Zhai et al. 2008; Ning et al. 2016). Regarding other CacyBP/SIP ligands, ERK1/2 and p38, it has been shown that CacyBP/SIP exhibits phosphatase activity towards these kinases (Kilanczyk et al. 2009; Topolska-Woś et al. 2015).

Recently, we have shown that CacyBP/SIP is present in the nucleus and that it interacts with a nucleolar protein NPM1 (Rosińska and Filipek 2018). NPM1 is an RNA binding protein involved in pre-rRNA processing, specifically, in the assembly of the 60 S large ribosomal subunit in the nucleolus (Okuwaki et al. 2021). It has also been suggested that NPM1 can serve as a shuttle protein delivering the ribosomal subunits to the cytoplasm (Jr Maggi et al. 2008). Considering this, we ventured to look if CacyBP/SIP, as a binding partner of NPM1, could also be involved in ribosome biogenesis and/or function. For that, we searched for ribosomal proteins (RPs) that could be potential CacyBP/SIP interacting partners. We performed mass spectrometry analysis using neuroblastoma NB2a cell lysate and found that, besides previously identified targets (e.g. tubulin, S100A6, NPM1), some RPs could also be CacyBP/SIP ligands. In this study we concentrated on the RPL6 protein since it was identified with a high quality score in mass spectrometry analyses. We applied various biochemical methods and in silico analysis, and confirmed the interaction of CacyBP/SIP with RPL6. Finally, we performed various analyses using NB2a cells with diminished CacyBP/SIP level and found that the protein may have an impact on protein synthesis.

Methods

Plasmids and proteins

The plasmid for silencing mouse CacyBP/SIP expression, pGPU6/Hygro-CacyBP/SIP-Mus-546, and a control plasmid, pGPU6/Hydro/shNC, were purchased (GeneDireX, Inc. Las Vegas, NV USA). The construction of plasmid for overexpression of CacyBP/SIP, p3xFLAG-CMV-10-CacyBP/SIP, was described by Schneider et al. (2007). The plasmids for overexpression of RPL6 and RPL6 C-terminal domain in NB2a cells were prepared as follows. Human RPL6 coding sequence was amplified using cDNA prepared from HEK293 cells and appropriate primers (Supporting information file, Tab. S1). The PCR product was cloned as a fusion with C-terminal Myc-tag in pcDNA3.1-Myc plasmid using restriction enzymes Hind III and Xho I. To create plasmid encoding RPL6 C-terminal domain (RPL6-ΔC), the above plasmid was used as a template in the PCR reaction with appropriate primers (Supporting information file, Tab. S1). The PCR product was treated with T4 polymerase to generate single stranded cohesive ends and the resulting DNA was used to transform *E. coli Xl1* cells (Li and Elledge 2012). Construction of the pET28a-CacyBP/SIP plasmid and purification of recombinant protein were described in (Topolska-Woś et al. 2015; Filipek et al. 2002). Briefly, His_6-tagged CacyBP/SIP was expressed in *E. coli BL21(DE3)* strain. Bacteria were cultured at 37°C in LB medium with kanamycin (50 µg/ml) until OD_{600} reached 0.7. Then, CacyBP/SIP expression was induced by addition of IPTG (0.4 mM final concentration) and the bacterial culture was continued for another 3 h at 37°C. The expressed His_6-tagged CacyBP/SIP was purified by gravity flow using TALON Co^{2+} metal affinity resin (Clontech, Takara Bio, San Jose, CA, USA) at RT, followed by removal of the His_6-tag with thrombin (Merck Millipore, Darmstadt, Germany). The protein was dialyzed against buffer containing 150 mM NaCl and 20 mM Tris-HCl, pH 8.4. Recombinant RPL6

protein was purchased (Antibodies-online GmbH, Aachen, Germany).

Culture of neuroblastoma NB2a cells, cell transfection, establishment of stable cell lines and heat shock

Mouse neuroblastoma NB2a cells were purchased (ATCC, Manassas, VA, USA). Cells were grown in EMEM (Eagle's Minimum Essential Medium) containing 10% fetal bovine serum (Gibco, Waltham, MA, USA), 26 mM sodium bicarbonate (Sigma-Aldrich, St. Louis, MO, USA), 100 U/ml penicillin and 100 µg/ml streptomycin (Sigma-Aldrich, St. Louis, MO, USA), 2 mM L-Glutamine (Sigma-Aldrich, St. Louis, MO, USA), and 0.25 µg/ml amphotericin B (Gibco, Waltham, MA, USA) at 37 °C under 5% CO_2. The medium was changed every 3 days and cells were passaged when confluent.

To obtain NB2a cell line with CacyBP/SIP knock-down, referred to as CacyBP/SIP-KD, and a proper control (Ctrl), 70% confluent NB2a cells were transfected with pGPU6/Hygro-CacyBP/SIP-Mus-546 or pGPU6/Hydro/shNC plasmid, respectively, using Lipofectamine2000 (Thermo Fisher Scientific, Waltham, MA, USA) according to manufacturer's instructions. The transfection mixture was added to the medium containing 5% (*w*/*v*) FBS without antibiotics. After 6 h, the medium was replaced with a complete one. After 48 h, hygromycin B (Sigma- Aldrich, St. Louis, MO, USA) was added at the final concentration of 100 µg/ml for selection of plasmid bearing cells. The hygromycin B supplemented medium (as above) was changed every 3 days. Cells were cultured in such conditions for about 30 days.

To obtain NB2a cells with transient overexpression of CacyBP/SIP with FLAG tag, NB2a cells were transfected with p3xFLAG-CMV-10-CacyBP/SIP or with control p3xFLAG-CMV-10 plasmid (Schneider et al. 2007) and cultured for 24 h. To obtain NB2a cells with transient overexpression of RPL6 or RPL6-C-terminal domain with Myc tag, NB2a cells were transfected with pcDNA3.1-Myc-RPL6 or pcDNA3.1-Myc-RPL6-ΔC plasmid, respectively, and cultured for 24 h.

Heat shock was applied as follows. Control (Ctrl) and CacyBP/SIP-KD NB2a cells, 70% confluent, were washed in PBS and placed in EMEM medium containing 5% FBS and no antibiotics. Culture dishes were sealed with parafilm and incubated in a water bath (JULABO GmbH, Seelbach/Germany) at 43 °C (heat shock) or at 37 °C (control) for 45 min. After heat shock, the cells were placed again in a fresh complete medium and were allowed to recover in a 5% CO_2 incubator (Heraeus Electronics, Hanau Germany) at 37 °C for 1, 4–24 h. Cells were then washed with PBS and incubated for 30 min at 4 °C in buffer containing: 25 mM Tris-HCl pH 7.5, 150 mM NaCl, 1 mM EDTA, 1 mM EGTA, 0.5% (v/v) IGEPAL, 1% (v/v) Triton X-100, supplemented with protease and phosphatase inhibitors (Roche Molecular Biochemicals, Mannheim, Germany). The cell lysate was then centrifuged at 14,000 (Eppendorf centrifuge 5417 R) for 20 min and protein concentration was estimated in the supernatant using Bradford (Bio-Rad, Hercules, CA, USA) and BSA (Serva, Heidelberg, Germany) as a standard protein. 40 µg of total protein was subjected to SDS–PAGE and Western blot.

Co-immunoprecipitation and mass spectrometry

For immunoprecipitation (IP) of CacyBP/SIP, NB2a cells were transfected with 3xFLAG-CMV-10-CacyBP/SIP or with 3xFLAG-CMV-10 (control) plasmid. After 24 h, cells were washed with ice-cold PBS and scraped with IP buffer (50 mM Tris pH 7.5, 150 mM NaCl, 1 mM EDTA, 1% Triton-X100) containing protease inhibitor. Cell lysates were then centrifuged for 10 min at 12,500 rpm (Eppendorf centrifuge 5417 R) at 4 °C and the supernatant was collected for further analysis.

Protein concentration was measured by the Bradford method as described above. Samples of 50 µg protein were kept as input. For IP, a portion of the supernatant containing 1000 µg of protein was added to 40 µl of anti-FLAG M2 agarose resin (Sigma-Aldrich, St. Louis, MO, USA) previously equilibrated by washing 3 times with IP buffer. The samples were then equalized to 1 mL with IP buffer and left on a rotor platform for 3 h at 4°C. After that time, 5% of protein sample (unbound fraction) was kept while the resin was washed five times with IP buffer. The unbound fraction and last wash were precipitated with acetone and subjected to SDS-PAGE. Depending on the output analysis, samples were then processed differently. For the Western blot analysis, the bound proteins were eluted from the resin by addition of 2 x Laemmli sample buffer and 10 min incubation with shaking at 50°C, followed by addition of DTT (1:10) and boiling for 5 min at 95°C with shaking. For mass spectrometry analysis, the resin was additionally washed 3 times with IP buffer without detergents and protease inhibitors (50 mM Tris pH 7.5, 150 mM NaCl, 1 mM EDTA). After that, beads were resuspended in 50 µL of 50 mM Tris-HCl, pH 8.0 and subjected to mass spectrometry in the Institute of Biochemistry and Biophysics, PAS, Warsaw, Poland (for details see the Supporting information file). Briefly, peptides were analyzed using an LC-MS system consisting of an Evosep One (Evosep Biosystems) coupled with an Orbitrap Exploris 480 mass spectrometer (Thermo Fisher Scientific, Waltham, MS, USA). The mass spectrometry proteomics data have been deposited to the ProteomeXchange Consortium *via* the PRIDE (Perez-Riverol et al. 2025) partner repository with

the dataset identifier PXD064560 and https://doi.org/10.6019/PXD064560". The proteins identified in cells expressing 3xFLAG-CMV-10-CacyBP/SIP were compared to the ones found in control 3xFLAG-CMV-10 - expressing cells (Tab. S2). Proteins fulfilling the following criteria were considered as CacyBP/SIP interactors: they were identified in at least two, out of three, experiments and had a three times higher sum of Mascot scores in 3xFLAG-CMV-10-CacyBP/SIP samples in comparison to the control ones.

Affinity chromatography

The coupling of purified recombinant CacyBP/SIP protein, obtained as described earlier (Filipek et al. 2002; Schneider et al. 2010) to CNBr-Sepharose (GE Healthcare) was carried out according to the procedure outlined by the manufacturer. At the same time a control resin with no coupled protein but blocked with Tris (CNBr-Sepaharose-empty), was prepared.

For affinity chromatography, NB2a cells were transfected with RPL6-Myc-tag or with RPL6 ΔC-Myc-tag plasmid. After 24 h, cells were washed with ice-cold PBS and scraped with IP buffer (50 mM Tris pH 7.5, 50 mM NaCl, 1 mM EDTA, 1% Triton-X100) containing protease inhibitors. Cell lysates were then centrifuged for 10 min at 16 000xg at 4 °C and the supernatant was collected for further analysis. Protein lysate was applied to CacyBP/SIP affinity resins and to the empty resin (as a control). After incubation on a rotating wheel for 1 h at 4 °C, the resins were extensively washed with the same buffer and then the bound proteins were eluted with the buffer containing 150 mM and 500 mM NaCl. Collected fractions were precipitated with acetone and analyzed by SDS-PAGE followed by Western blot using monoclonal anti-c-Myc antibody.

SDS-PAGE and western blot

Proteins from the lysate or protein fractions from IP were separated on 10% SDS gel according to the Laemmli procedure (Laemmli 1970) and transferred onto nitrocellulose membrane (0.45 µm) (Bio-Rad, Hercules, CA, USA) using wet Transfer System (Bio-Rad, Hercules, CA, USA). Membranes were blocked at RT for 1 h in TBS-T (50 mM Tris, 200 mM NaCl, pH 7.5, 0.05% Tween-20) containing 5% fat-free milk and then incubated overnight with: rabbit polyclonal anti-CacyBP/SIP (1:1000) (#3354, Cell Signaling Technology, Danvers, MA, USA), rabbit polyclonal anti-RPL6 (1:500) (#PA5-30217, Thermo Fisher Scientific, Waltham, MS, USA), mouse monoclonal anti-c-Myc (1:500) (#sc-40, Santa Cruz Biotechnology, San Diego, USA) or rabbit polyclonal anti-Hsp70 (1:700) (# SPA 812, Enzo Life Sciences, New York, NY, USA) antibody. After washing, 3 times for 10 min with TBS-T, membranes were incubated for 1 h at RT with secondary goat anti-rabbit IgG antibody conjugated to HRP (#674371, MP Biomedicals, Irvine, CA, USA), diluted 1:10000. The mouse monoclonal anti-β-actin horseradish peroxidase (HRP)-conjugated antibody (#A3864, Sigma-Aldrich, St. Louis, MO, USA), diluted 1:10000, was used to monitor protein loading. The membrane was developed with ECL plus (New English Biolabs, Ipswich, MA, USA). The signal intensity was calculated using an Ingenius densitometer (Syngene International Limited, Bengaluru, Karnataka, India) and the Gene Tools software (Syngene, Cambridge, UK). β-actin served as a reference protein.

In the case of Western blot performed on fractions from sucrose gradient centrifugation, the nitrocellulose was blocked overnight at 4°C in 5% fat-free milk in TBS-T buffer followed by incubation for 5 h at RT with rabbit polyclonal anti-CacyBP/SIP antibody diluted 1:2000 (A302-905 A, Bethyl Laboratories, Montgomery, TX, USA). Then, the membrane was developed as described above. The membrane was subsequently washed and incubated for 5 h at RT with anti-RPL6 antibody diluted 1:500 (#PA5-30217, Thermo Fisher Scientific, Waltham, MS, USA) and developed in the same way as previously described.

RT-qPCR analysis

Total RNA was isolated using Universal RNA Purification kit (EURx, Gdańsk, Poland). RNA (1 µg) was then reverse-transcribed using NG dART RT kit (EURx, Gdańsk, Poland). The relative mRNA level of CacyBP/SIP was assessed by RT-qPCR using the SYBR Green system with 18 S rRNA as the reference standard. The sequences used for CacyBP/SIP and 18S rRNA are listed in Supporting information file, Tab. S1. The results were analyzed by absolute quantification with a relative standard curve and normalized to 18S rRNA *via* the comparative ΔΔCt method.

ELISA

Wells of a 96-well plate were coated with commercially purchased RPL6 (Antibodies-online GmbH, Aachen, Germany) or bovine serum albumin (BSA) (Serva, Heidelberg, Germany) (400 ng/well) in 50 µl of Coating Buffer (CB) pH 8.1 containing 100 mM Na_2HPO_4 and 100 mM NaH_2PO_4. After overnight incubation at 4 °C, the solution was discarded, and the wells were washed with PBS-T (PBS + 0.05% Tween-20). The remaining absorption sites were blocked for 3 h at RT with 10% BSA. Then, wells were washed with Reaction Buffer (RB) containing 10 mM Tris-HCl pH 7.5, 50 mM NaCl, 5 mM $MgCl_2$, 5% (v/v) glycerol, 2 mg/ml BSA, 2 mM DTT and 0.05% (v/v) Triton X-100.

After that increasing concentrations (0 to 3.52 µM) of recombinant CacyBP/SIP in 50 µl of RB were applied. After overnight incubation at 4 °C, the wells were washed with PBS-T and the primary rabbit polyclonal antibody against CacyBP/SIP (#3354, Cell Signaling Technology, Danvers, MA, USA) diluted 1:500 in 10% BSA in PBS-T was applied for 3 h at RT. Following the washing procedure with PBS-T, incubation with secondary HRP-conjugated anti-rabbit antibody (#674371, MP Biomedicals, Irvine, CA, USA) diluted 1:7000 in 10% BSA in PBS-T was carried for 2 h at RT. After the final wash with PBS-T, the bound antibodies were detected colorimetrically using the TMB peroxidase EIA substrate (Millipore, Darmstadt, Germany) according to the manufacturer's instructions. The reaction was stopped with 1 M sulfuric acid and absorbance was measured at 450 nm using a microplate reader (Thermo Fisher Scientific, Waltham, MA, USA).

Proximity ligation assay (PLA)

In order to visualize the CacyBP/SIP-RPL6 complex in the cell, a PLA assay was performed. This assay allows for visualization of protein-protein interactions since the fluorescence signal is generated only if the protein molecules in the cell are within a distance no longer than 40 nm from each other. To perform this assay a PLA kit (Sigma-Aldrich, St. Louis, MO, USA) was applied and NB2a cells cultured on coverslips were used. Cells were fixed with 3% (w/v) paraformaldehyde in the PBS buffer for 20 min at RT. After washing with PBS, cells were permeabilized for 4 min at 4 °C in the same buffer containing 0.1% (v/v) Triton X-100. All steps were performed according to manufacturer's instructions using reagents (except primary antibodies) and buffers provided in the PLA kit. After blocking with Duolink Blocking Solution for 1 h at 37 °C, the reaction was carried out for 1.5 h at RT with the following primary antibodies: rabbit polyclonal anti-RPL6 (#PA5-30217, Thermo Fisher Scientific, Waltham, MS, USA) diluted 1:500 and mouse monoclonal anti-CacyBP/SIP (# sc-166163, Santa Cruz Biotechnology, San Diego, USA) diluted 1:200. After washing, the incubation with anti-rabbit PLA plus and anti-mouse PLA minus probes (1:4) was implemented for 1 h at 37 °C in a humidity chamber. Following the ligation and amplification steps, the coverslips were immobilized on microscopic slides with mounting medium. In the negative control the ligation step was omitted. Cells were analyzed under the Zeiss Spinning Disc confocal microscope (Carl Zeiss GmbH, Oberkochen, Germany) equipped with a 63×oil objective.

Sucrose gradient centrifugation/polysome profiling

Mouse neuroblastoma NB2a cells were grown on 15 cm plates (9 such plates were used in each experiment) until reaching 70–90% confluency, and then treated with cycloheximide (Sigma-Aldrich, St. Louis, MO, USA) for 5 min at 37ºC to freeze active translation. Then, the plates were transferred onto ice, the medium was removed, and cells were gently washed with ice-cold PBS containing cycloheximide (100 µg/ml final concentration). Cells were harvested by scraping, transferred to a 15 ml Falcon tube and centrifuged at 800 rpm (Eppendorf centrifuge 5417 R) for 6 min at RT. The supernatant was discarded, and cells were resuspended in PBS (1 ml PBS for cells harvested from 1 plate). Then, DSP (dithiobis succinimidyl propionate) (Thermo Fisher Scientific, Waltham, MA, USA) was added to a final concentration of 0.3 mM and incubation was continued for another 30 min at RT with continuous rotation on a roller mixer (Techniprot, Pruszków, Poland). In the next step, 1 M Tris-HCl, pH 7.5 was added to the mixture to a final concentration of 50 mM and incubation on the roller was continued for 15 min at RT. Then, the mixture was centrifuged at 800 rpm (Eppendorf centrifuge 5417 R) for 7 min at RT and the pellet was resuspended in 1350 µl of the lysis buffer containing 20 mM Tris-HCl pH 7.4, 100 mM KCl, 5 mM $MgCl_2$, 1% Triton X-100, cycloheximide (100 µg/ml final concentration), protease inhibitor cocktail and RNase inhibitor (Merck Millipore, Darmstadt, Germany) (100 U/µl final concentration). The mixture was transferred to a 1.5 ml Eppendorf tube, incubated for 5 min on ice and centrifuged for 15 min at 14,000 rpm (Eppendorf centrifuge 5417 R) at 4ºC. The pellet was discarded, and the supernatant was transferred to a new tube, incubated with RQ1 RNase-free DNase (Promega, Madison, Wisconsin, USA) (0.01 U/µl final concentration) for 10 min at RT and used for a sucrose gradient centrifugation. In the meantime, the solutions of 10% and 50% sucrose were prepared in polysome buffer containing 20 mM HEPES-KOH, pH 7.4, 100 mM KCl, 5 mM $MgCl_2$, cycloheximide (100 µg/ml final concentration) and protease inhibitor cocktail. Equal volumes (5.5 ml) of 10% and 50% sucrose solutions were added to the Open-Top Thinwall Ultra-Clear tube (Beckman Coulter, Indianapolis, Indiana, USA) and the 10–50% sucrose gradients were prepared using the Gradient Station (BioComp Instruments Ltd., Fredericton, NB, Canada). Subsequently, 500 µl of the supernatant was carefully layered on top of the 10–50% sucrose gradient. Two tubes were subjected to ultracentrifugation at 28,000 rpm in a Beckman SW41 rotor for 5 h at 4ºC. Following ultracentrifugation, the tubes were kept on ice for immediate fractionation. The content of each tube was divided into separate fractions, each containing 0.55 mL. Simultaneously, continuous absorbance profiles

of the gradients at 260 nm were monitored using BioComp TRiAX flow cell (BioComp Instruments Ltd., Fredericton, NB, Canada). Before analysis by Western blot, proteins from each fraction were precipitated with 96% ethanol (9:1 v/v) overnight at -70º C, centrifuged at 14,000 rpm (Eppendorf centrifuge 5417 R) for 30 min at 4ºC and resuspended in Laemmli sample buffer containing DTT (10 mM final concentration). Proteins were separated in 12.5% polyacrylamide gel according to the Laemmli procedure (Laemmli 1970) and then transferred to a 0.45 µm nitrocellulose membrane using a wet transfer system (Bio-Rad, Hercules, CA, USA).

Protein synthesis assay

The effect of CacyBP/SIP knock-down on nascent protein synthesis in cultured NB2a cells was examined using Click-iT® Plus OPP Protein Synthesis Assay Kits (Life Technologies, Carlsbad, CA, USA) in accordance with the manufacturer's instructions. Control or CacyBP/SIP-KD NB2a cells were grown in poly-l-lysine (Sigma-Aldrich, St. Louis, MO, USA) coated wells in a cell culture chamber (Biologix, Jinan, Shandong, China) at 37 °C under 5% CO_2 for 24 h until reaching 60–70% confluency. After removing the medium, cells were incubated with the OPP reagent at the final concentration of 20 µM for 30 min at 37ºC. Then, cells were washed with PBS, followed by fixation with 4% paraformaldehyde for 20 min at RT. After washing with PBS, cells were permeabilized with 0.1% Triton X-100 for 15 min at RT, washed again with PBS and exposed to a Click-iT Plus OPP reaction cocktail for 30 min at RT. Next, cells were washed with Click-iT Reaction Rise buffer and PBS, followed by incubation with 3% BSA for 1 h at RT. In the subsequent step cells were incubated overnight at 4ºC with rabbit anti-CacyBP/SIP antibody (#A302-905 A, Bethyl Laboratories, Montgomery, TX, USA) diluted 1:200 in PBS containing 1% BSA. The reaction with secondary anti-rabbit Alexa Fluor 555 antibody (#A21428, Invitrogen, Carlsbad, CA, USA) diluted 1:500 in PBS containing 1% BSA was carried out at RT for 1 h. After final washing with PBS, the coverslip was mounted on the slide with VectaShield (Vector Laboratories, Burlingame, CA, USA). Fluorescence staining was analyzed under a Leica microscope (TCS SP8; Leica Microsystems GmbH, Wetzlar, Germany) using a 63x/1.4 oil immersion objective. Several microscopic images, with 150 cells in total, were analyzed and the percentage of cells with enhanced OPP staining was calculated for both control and CacyBP/SIP-KD cell lines.

ER tracker assay

The influence of CacyBP/SIP knock-down on endoplasmic reticulum (ER) network in NB2a cells was studied using ER-Tracker Blue-White DPX (Molecular Probes, Eugene, OR, USA) in accordance with the manufacturer's instructions. Stably transfected NB2a cells, control or CacyBP/SIP-KD, were cultured on poly-l-lysine coated wells in the chamber at 37 °C under 5% CO_2 for 24 h until reaching 60–70% confluency. After washing with medium, cells were incubated with ER-Tracker dye at the final concentration of 1 µM for 30 min at 37 °C. Next, cells were washed with fresh medium and with PBS and fixed with 4% paraformaldehyde for 20 min at RT and washed with PBS. Finally, the coverslip was mounted on the slide with VectaShield. Fluorescence staining was analyzed under a Leica microscope (TCS SP8; Leica Microsystems GmbH, Wetzlar, Germany) using a 63x/1.4 oil immersion objective. The intensity of ER staining was measured for 50 cells in each cell line, control and CacyBP/SIP-KD, using the Image J software (NIH, Bethesda, MD, USA).

In silico analysis of CacyBP/SIP - RPL6 interaction

In silico protein-protein docking studies of the CacyBP/SIP-RPL6 interaction were performed using the ClusPro 2.0 server and the YASARA-Structure v. 24.4.10 software. The 3D structures of mouse CacyBP/SIP (UniProt ID: Q9CXW3) and mouse RPL6 (UniProt ID: P47911) were obtained from the AlphaFold Database (Varadi et al. 2024). The three domains of CacyBP/SIP and the C-terminal domain of RPL6, as the only well-defined domains, were extracted using YASARA-Structure. The C-terminal domain of RPL6 (residues 148–283) represents a rigid structure except for a long flexible loop consisting of residues 226–250. This loop was removed from the domain before protein-protein docking. The N-terminal domain of CacyBP/SIP was used in a dimeric form since it was found to be responsible for CacyBP/SIP dimer formation.

The N-terminal domain in the form of a dimer (based on crystal structure PDB ID:2A26, residues 3–48), the middle domain (residues 71–180), and the C-terminal domain (residues 186–229) of CacyBP/SIP were docked separately to the C-terminus of RPL6 using the ClusPro server (Desta et al. 2020) to explore the potential binding interactions. This server rotates the C-terminal domain of RPL6 with tens of thousands of rotations in the proximity of CacyBP/SIP domains and generates the most optimal models based on weighted scores. The resulting structures were clustered and the central structures of these clusters were scored. The top scored models obtained from the ClusPro server were subsequently analyzed using YASARA-Structure 24.4.10

(Krieger and Vriend 2015) to calculate both the contact surface and the binding energy. Before calculations, the structures were optimized to remove short contacts between atoms. The procedure consisted of three steps: (1) caps were added to terminal residues of particular domains to prevent artificial effects of charged endings; (2) local steepest descent energy minimization was conducted to remove bumps, and (3) simulated annealing was done to optimize contacts between side chains of amino acid residues. The last two steps were conducted using the NOVA2 forcefield (Krieger et al. 2002) in YASARA-Structure, which is suitable for minimizations and simulations in vacuum by using the implicit solvent. Not only the potential energies were calculated but also the solvation terms to compensate for the calculations in vacuum. The formula for the interaction energy between domains is presented below. For this formula, the higher the calculated value, the more favorable the interaction energy.

$$\left(E^{pot}_{domain\ 1} + E^{solv}_{domain\ 1}\right) + \left(E^{pot}_{domain\ 2} + E^{solv}_{domain\ 2}\right) - \left(E^{pot}_{domains\ 1+2} + E^{solv}_{domains\ 1+2}\right)$$

The contact surface of the top ranked models from ClusPro server was calculated using the Solvent Accessible Surface Area (SASA) in YASARA-Structure based on the formula below.

$$\frac{SASA_{CacyBP/SIP} + SASA_{RPL6} - SASA_{Docked\ model}}{2}$$

The best structure, composed of the interacting C-terminal domains of both proteins, was used for reconstruction of the full structure of the complex using the AlphaFold models of individual proteins (Varadi et al. 2022). The structure of the complex was subjected to molecular dynamics (MD) simulations. The protocol used for preparation and initial steps of MD simulation was the same as used in (Jarmula et al., 2017), except: (1) the solvation with octahedron box of TIP3P water molecules was set up at the distance of 10 Å away from the outer protein wall, (2) a gradual heating from 0 to 300 K was carried out in three 10 ps intervals (0–100 K, 100–200 K and 200–300 K), followed up by a 2 ns-long equilibration and, finally, three replicas of 300 ns-long data collection simulations, (3) the temperature was controlled by a Berendsen weak-coupling algorithm and pressure by isotropic position scaling with Berendsen barostat (Berendsen et al. 1984), (4) a 1-fs integration time step has been used and (5) all MD simulations were performed with pmemd.cuda from Amber 22 package (Case et al. 2022) using the sander program in each replica. The main chains of the C-terminal domains of both proteins were restrained (restraint value of 5 kcal/mol*Å^2) during MD simulations to keep contact between both proteins. Clustering of the obtained structures was done in cpptraj program.

Calculations of the contact surface and the interaction energy for separated domains of CacyBP/SIP and RPL6 of the structures from all replicas of MD simulations were done in YASARA-Structure using the NOVA2 forcefield as described above. To test the possibility of CacyBP/SIP to RPL6 binding in the ribosome, the crystal structure of a complete ribosome containing both the 60 S and 40 S subunits (PDB id: 7CPU) (Li et al. 2022) was used. The superimposition was done in YASARA-Structure by overlaying the C-terminal domains of RPL6 from the CacyBP/SIP-RPL6 complex and the ribosomal RPL6.

Table 1 List of ribosomal proteins (RPs) potentially interacting with CacyBP/SIP

#	Entry name	Protein name	Gene name
1	RPL6_MOUSE	60 S ribosomal protein L6	RPL6
2	RS4X_ MOUSE	40 S ribosomal protein S4	RPS4
3	RL7A_ MOUSE	60 S ribosomal protein L7a	RPL7a
4	RL3_ MOUSE	60 S ribosomal protein L3	RPL3
5	RS15A_ MOUSE	40 S ribosomal protein S15a	RPS15a

Statistical analysis

Each experiment was performed in at least 3 biological repetitions. Data were analyzed in Prism 6 (GraphPad Software). The results from the ELISA assay were analyzed using a two-way ANOVA. Multiple comparisons were performed using Šidák's post-hoc test ($\alpha = 0.05$). To check the significance of differences observed in Western blot and immunofluorescence, between NB2a control (Ctrl) and CacyBP/SIP knock-down (CacyBP/SIP-KD) cells, the Student's *t*-test was applied. The significance of mean comparison is annotated as follows: *$p \leq 0.05$, **$p \leq 0.01$, ***$p \leq 0.001$ and **** $p \leq 0.0001$.

Results

Identification of RPL6 as CacyBP/SIP ligand and analysis of their interaction in vitro

At first, we searched for ribosomal proteins that might interact with CacyBP/SIP. For that, we performed immunoprecipitation using protein lysate obtained from NB2a cells overexpressing CacyBP/SIP-3xFLAG or 3xFLAG alone (control). Elution fractions from anti-FLAG agarose were then analyzed by mass spectrometry (Supporting information file, Tab. S2). This analysis revealed that several ribosomal proteins (RPs) could be potential CacyBP/SIP targets (Table 1).

Moreover, Gene Ontology (GO) enrichment analysis, performed using ProteoRE bioinformatics software (Mehta et al. 2023), demonstrated that proteins identified by mass spectrometry and classified according to biological process (BP) and cellular component (CC) were mostly localized to ribosome, polysome, cytosolic ribosome, and intermediate filament and involved in biogenesis assembly and organization of the ribonucleoprotein complex (Fig. S1). These results indicate a strong association of CacyBP/SIP with ribosome-related processes and functions.

RPL6 was one of the proteins with the best quality scores identified in three mass spectrometry analyses. Thus, we performed immunoprecipitation, as described above, and analyzed fractions from the anti-FLAG resin by Western blot. As shown in Fig. 1A, the band corresponding to RPL6 was detected by anti-RPL6 antibody in the elution fraction of the lysate prepared from CacyBP/SIP-3xFLAG overexpressing, but not that from control cells.

To further confirm the interaction between CacyBP/SIP and RPL6, an ELISA assay with the use of recombinant proteins, was performed. The reaction was carried out in a 96-well plate coated with RPL6 or BSA (control) and then the immobilized proteins were incubated with increasing concentrations of CacyBP/SIP. The amount of CacyBP/SIP bound to RPL6 was estimated using an anti-CacyBP/SIP antibody. Detection of CacyBP/SIP-RPL6 complexes was performed using the colorimetric method. As illustrated in Fig. 1B much higher absorbance was registered when CacyBP/SIP was added to the wells coated with RPL6 when compared to those coated with BSA. Results of this experiment confirm the interaction between CacyBP/SIP and RPL6 and, moreover, show that the interaction is direct.

Docking of separate domains of CacyBP/SIP and RPL6

For the protein-protein docking method we used all three domains of CacyBP/SIP (N-terminal, middle and C-terminal) separately since they are connected by flexible linkers. Since CacyBP/SIP dimerizes through the N-terminal domain, we used a crystal structure of this domain in a dimeric form (Topolska-Woś et al. 2016). For RPL6, we used only its C-terminal domain as it is the sole structurally stable domain of this protein. We confirmed the interaction of CacyBP/SIP with the RPL6 C-terminal domain (residues 135–288) using affinity chromatography (Fig. S2). Protein-protein docking was conducted in ClusPro 2.0 server, and the obtained parameters of binding (number of cluster members and the weighted score) are shown in Table 2.

In both models of CacyBP/SIP N-terminal dimer, RPL6 could bind, albeit weakly, to each of the monomers, so dimerization had no influence on the binding. The weighted scores were the best for docking of the C-terminal domain of CacyBP/SIP. The same domain was indicated as the best by the binding energy calculated in the YASARA-Structure program. Then, we analyzed the two best models (model 0 and model 1) since they had a similar score and a similar number of structures in both clusters. Both models are shown in Fig. 2A with a superimposed C-terminal domain of RPL6, to illustrate relative positions of the C-terminal domain of CacyBP/SIP. Model 1 is rotated about 60° in relation to model 0 but the binding occurs on the same side of the C-terminal domain of RPL6. The long flexible and unstructured loop of the C-terminal domain of RPL6 (residues 226–250), which was not used for docking, does not interfere with the binding of the C-terminal domain of CacyBP/SIP (Fig. 2A), so the models are correct also for the whole RPL6 domain. The other domains of CacyBP/SIP in the initial model of this protein are located far from its C-terminal domain, so they do not interfere with the binding either.

Although the weighted score for model 0 is better than for model 1, the contact surface is larger for model 1. In addition, the calculated binding energy in YASARA-Structure favors model 1. However, the hydrophobic interactions are not adequately accounted in the binding energy because they are entropic in nature. Therefore, we analyzed hydrophobic interactions in the interface between C-terminal domains of both proteins in model 0 and model 1. It turned out that such interactions were much more extensive in model 0 and involved residues L196, I199, I211, and W215 of the C-terminal domain of CacyBP/SIP, and L161, F201, and I203 of the C-terminal domain of RPL6 (Fig. 2B). For model 1, the hydrophobic contact involves less residues: L196, I211, and W215 of the C-terminal domain of CacyBP/SIP, and only F201 of the C-terminal domain of RPL6. Based on the above analysis we decided to use model 0 for further studies - it is also in agreement with the weighted score value which is better for model 0.

Molecular dynamics of the CacyBP/SIP-RPL6 complex and fitting of CacyBP/SIP to RPL6 in the ribosome

The whole-length proteins were reconstructed based on model 0 contact of their C-terminal domains presented in Fig. 2B. The whole structure of the CacyBP/SIP-RPL6 complex is presented in Fig. 3A. The conducted molecular dynamic (MD) simulations in three replicas provided structures, which were clustered within each replica. The central structures from the most populated clusters for each replica are shown in panels B-D in Fig. 3. For replica 1 (Fig. 3B) there are three additional sites of interactions between RPL6 and CacyBP/SIP apart from the contact between

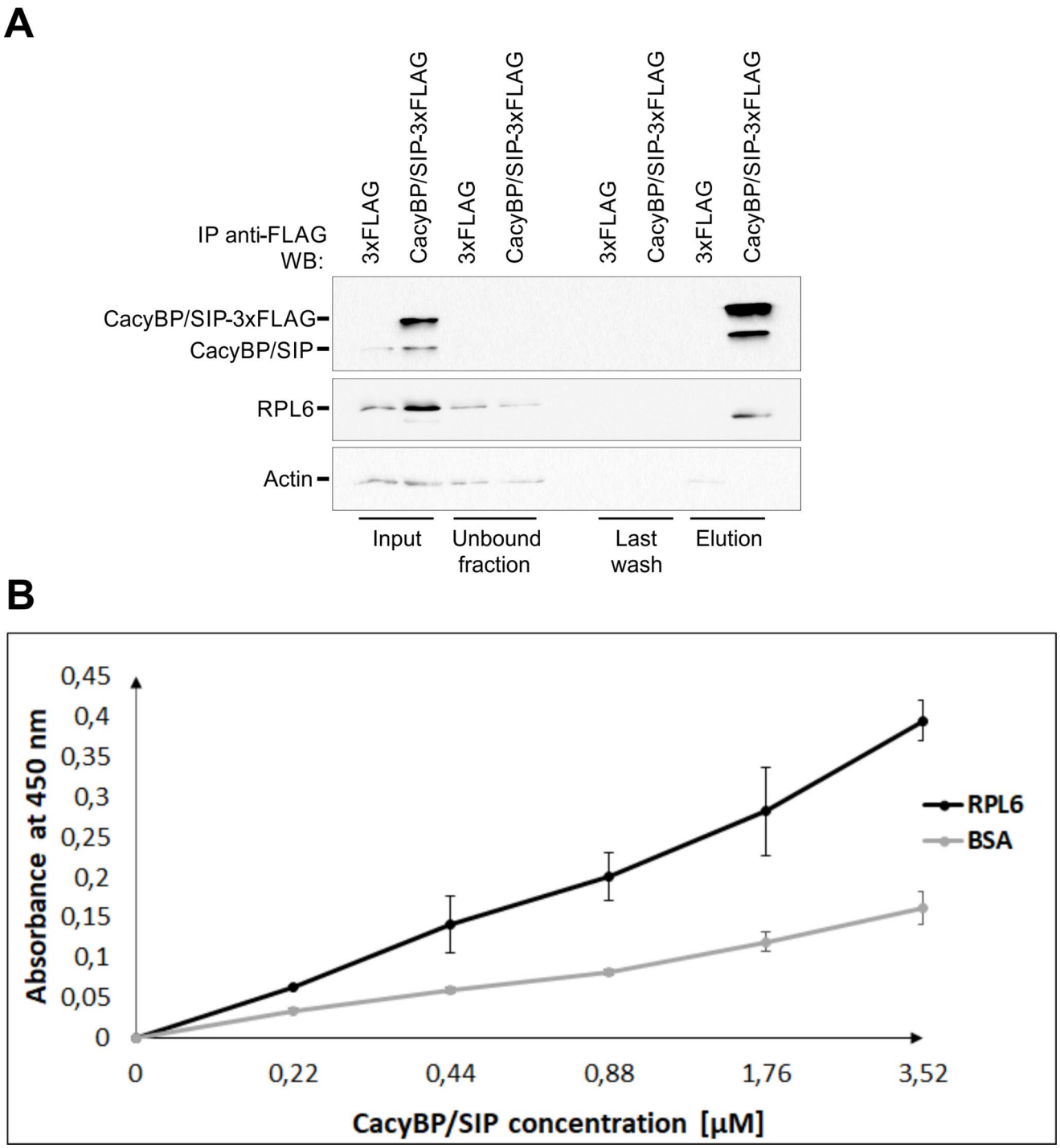

Fig. 1 (**A**) Co-immunoprecipitation of endogenous RPL6 with CacyBP/SIP-3xFLAG in NB2a cell lysate. The assay was performed using anti-FLAG agarose resin. Proteins in the elution fractions were analyzed by Western blot with anti-RPL6 or anti-CacyBP/SIP antibodies and actin serving as a control. RPL6 band is detected only in the elution fraction from the lysate of cells transfected with CacyBP/SIP-3xFLAG plasmid and not with control plasmid. (**B**) Binding of CacyBP/SIP to RPL6 assessed by ELISA. Purified recombinant proteins were applied and detection was performed with the use of anti-CacyBP/SIP antibody. Black and grey curves represent wells coated with RPL6 and BSA, respectively. Data ($n=3$) are presented as mean ± SD. Two-way ANOVA with a Šídák's multiple comparison test was used for analysis

Table 2 The calculated parameters of interaction of separate domains of CacyBP/SIP docked to the C-terminal domain of RPL6. The best models, based on the weighted score, are shown in bold

Model	CacyBP/SIP domain	ClusPro 2.0 Cluster members	ClusPro 2.0 Weighted Score	Contact surface [Å^2]	Binding Energy [kJ/mol]
0	N-term. dimer	149	-370.8	619.0	1398.0
1	N-term. dimer	113	-369.8	590.8	1467.7
0	Middle domain	153	-507.0	1074.4	2712.7
1	Middle domain	89	-529.5	881.7	2207.1
0	**C-term. domain**	**120**	**-646.1**	**817.5**	**2299.4**
1	**C-term. domain**	**114**	**-624.0**	**861.8**	**2514.3**

their C-terminal domains: (1) the C-terminus of CacyBP/SIP and residues 122–149 of RPL6 located in close proximity to the C-terminal domain of RPL6 (ionic interactions R122-F229(COO$^-$), K138-E228, R147-D226, R149-E217, and the π-π interaction Y123-F229; order of residues: RPL6-CacyBP/SIP), (2) a small contact involving the R112 residue from the middle domain of CacyBP/SIP and the residues from the long loop of the C-terminal domain of RPL6 (ionic interaction D242-R112) and (3) a small cluster involving a single R26 residue from the N-terminal domain of CacyBP/SIP and the residues from RPL6 located just before its C-terminal domain (N287/Y290-R26). The structure from replica 2 (Fig. 3C) contains only two additional areas of interactions: (1) the C-terminus of CacyBP/SIP and residues 102–150 of RPL6 that form a small subdomain (a cluster of residues linked by ionic interactions and hydrogen bonds K102/R113/R122/R146-Q222/E225/D226, ionic interaction R147-E228, and a hydrogen bond S150-F229(COO$^-$)) and (2) a residue from the middle domain of CacyBP/SIP (R112) and another residue from a linker between the middle and the C-terminal domain (Y182), and residues from the C-terminal domain of RPL6 (ionic interactions in a cluster E239/D242-R112, and the cation-π interaction K247-Y182). Finally, the structure from replica 3 (Fig. 3D) also contains two additional areas of interactions: (1) the C-terminus of CacyBP/SIP and residues 91–123 of RPL6 (ionic interactions K91/R122-F229(COO$^-$), and the π-π interaction Y123-F229), which form a small subdomain but a less compact one than that of replica 2 and (2) residues from the middle domain of CacyBP/SIP and residues from the long loop of the C-terminal domain of RPL6 (ionic interactions and hydrogen bonds: D242-R112/Q169, K245-E173 and K247-E178). The surface contacts and the binding energies between CacyBP/SIP domains and RPL6 are shown in Table 3. The largest contact surface and the highest binding energy are associated with the C-terminal domain of CacyBP/SIP, however, its middle domain, especially in replica 3 complex (Fig. 3D), also interacts strongly with RPL6 but only with the long loop of RPL6 C-terminal domain.

As it can be seen in Fig. 4A, RPL6 is located on top of the ribosomal 60 S subunit with most of its structure accessible from the outside. The long loop of the C-terminal domain of this protein does not interact with other ribosomal components in the crystal structure (PDB id: 7CPU) (Li et al. 2022).

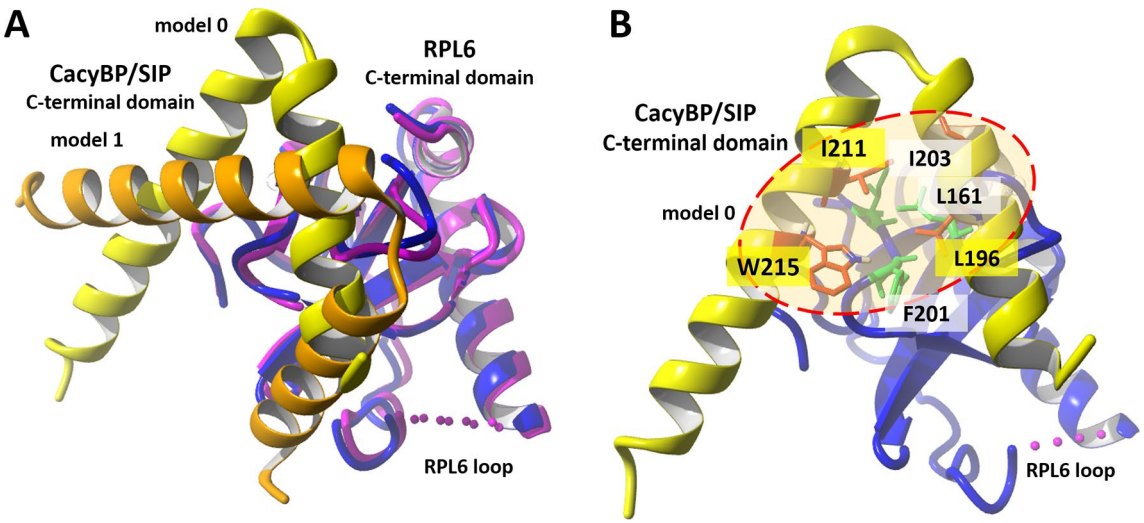

Fig. 2 Interaction of the C-terminal domains of CacyBP/SIP and RPL6. (**A**) Two best models of the C-terminal CacyBP/SIP domain (model 0 in yellow and model 1 in orange) are shown with a superimposed C-terminal domain of RPL6. (**B**) A cluster of interacting hydrophobic residues of model 0 (residues from the C-terminal domain of CacyBP/SIP are shown in orange color while those of the C-terminal domain of RPL6 in lime). The unstructured, long flexible loop of the C-terminal domain of RPL6 is indicated by purple dots. Labels for interacting residues are shown on a transparent yellow background for CacyBP/SIP and on a white one for RPL6

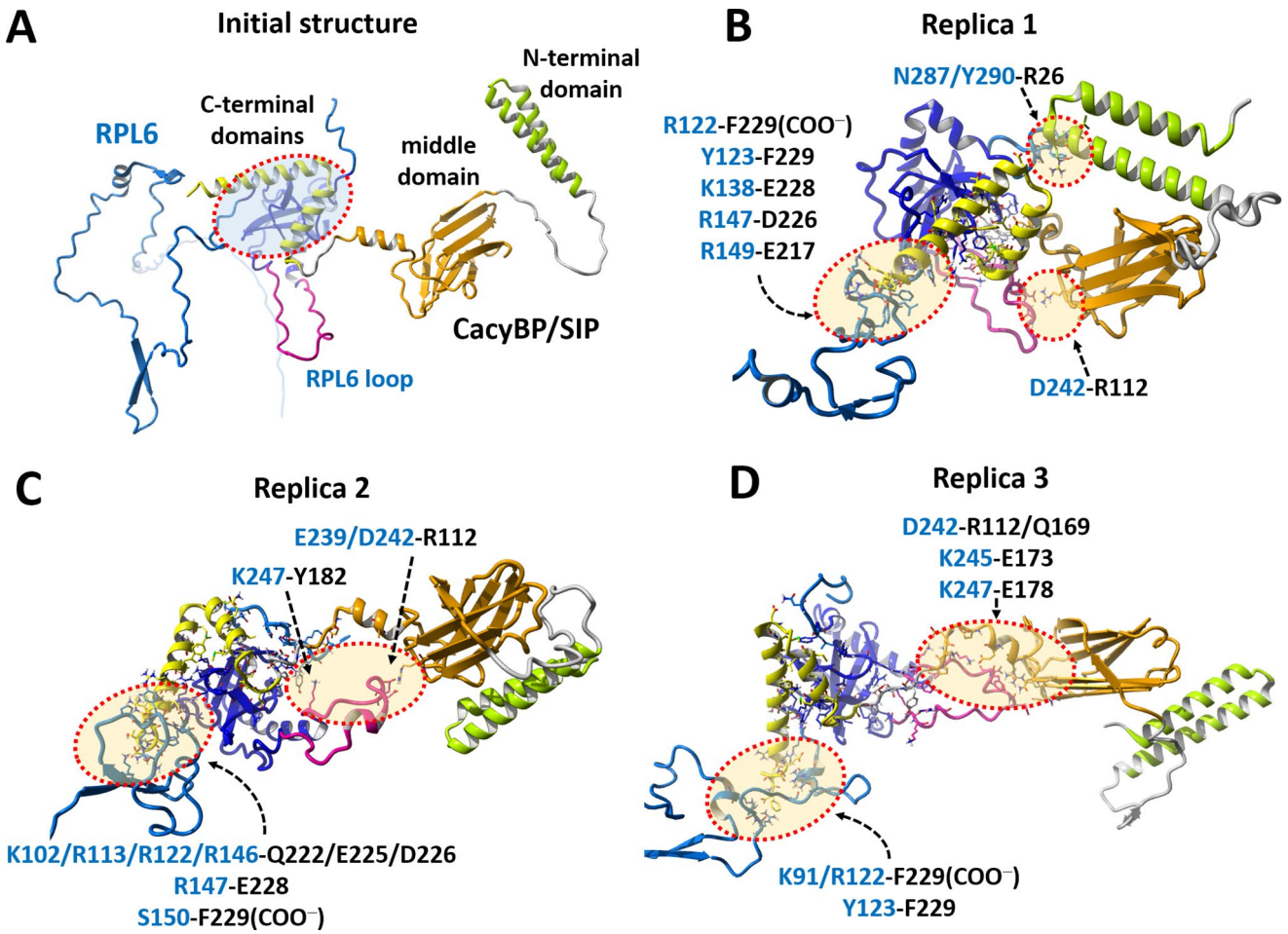

Fig. 3 Interaction of full length CacyBP/SIP and RPL6. (**A**) Initial complex after reconstruction of the structures of full length proteins based on the contact between the C-terminal domains. This contact is marked by a blue transparent area. RPL6 is shown in blue. Long flexible loop in the C-terminal domain of RPL6 is colored in pink. Domains of CacyBP/SIP are colored in yellow (C-terminal domain), orange (middle domain) and green (N-terminal domain). (**B**) The structure of CacyBP/SIP-RPL6 complex after 300 ns MD simulation (replica 1). (**C**) The structure of CacyBP/SIP-RPL6 complex after 300 ns MD simulation (replica 2). (**D**) The structure of CacyBP/SIP-RPL6 complex after 300 ns MD simulation (replica 3). Contacts other than these between the C-terminal domains are marked by orange transparent areas. The major interactions in these contacts are displayed. Residue labels in RPL6 are in blue

Table 3 Parameters of interaction (contact surface and interaction energy) between separate domains of CacyBP/SIP and the C-terminal domain of RPL6 for structures obtained from MD simulations conducted in three replicas

Replica	CacyBP/SIP domain	Contact surface [Å^2]	Interaction energy [kJ/mol]
1	N-terminal domain	198.6	383.7
1	Middle domain	424.6	946.1
1	C-terminal domain	1651.4	4725.4
2	N-terminal domain	0.0	2.4
2	Middle domain	356.6	792.3
2	C-terminal domain	1657.6	5450.2
3	N-terminal domain	0.0	7.7
3	Middle domain	546.6	1644.4
3	C-terminal domain	1590.3	4835.1

To check the potential interaction of CacyBP/SIP with ribosomal RPL6 we docked the replica 3 complex onto the crystal structure of the C-terminal domain of RPL6 (Fig. 4B). In this superimposition the C-terminal domain of CacyBP/SIP overlaps with other ribosomal proteins. To make the complex feasible we took out the C-terminal domain of CacyBP/SIP. This move was possible due to the presence of a long and flexible linker between the middle- and C-terminal domains of CacyBP/SIP (Fig. 4C). After C-terminal domain withdrawal, the interactions of the CacyBP/SIP middle domain and the long loop of the C-terminal domain of RPL6 remained the same as in replica 3 complex. The conformation of the RPL6 C-terminal domain long loop in replica 3 complex is slightly different from its conformation in the crystal structure but the interactions with the CacyBP/SIP middle domain are still feasible since this loop is free and

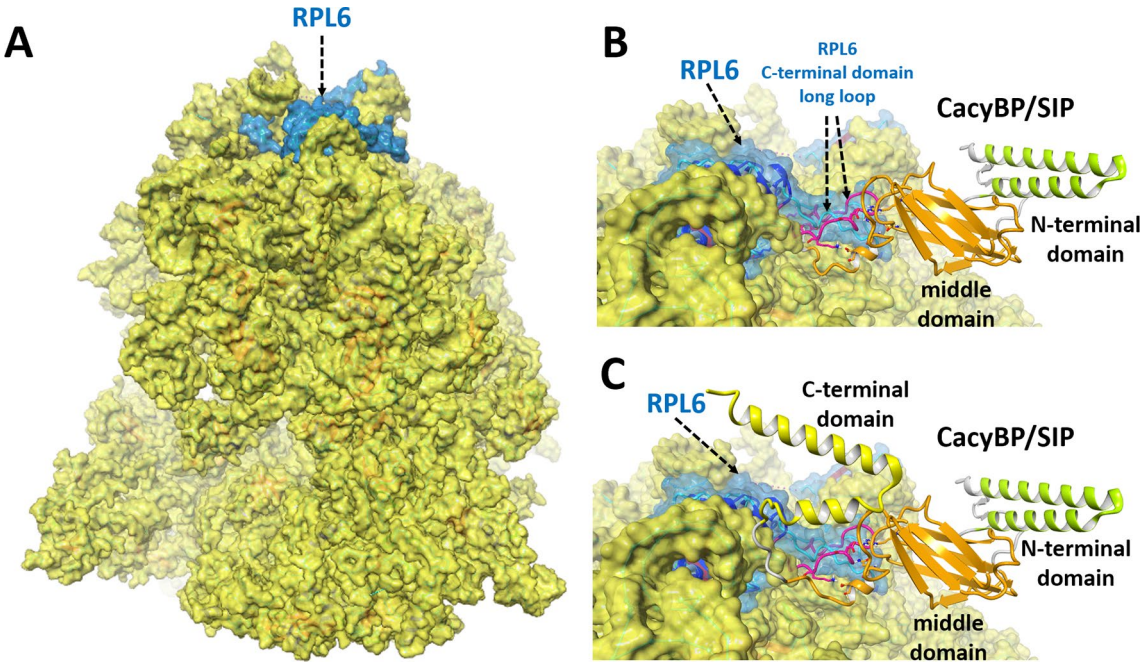

Fig. 4 Position of RPL6 in the ribosome and potential interaction with CacyBP/SIP. (**A**) Ribosome, shown in yellow surface (PDB id: 7CPU), and location of RPL6 on its top (shown in blue surface). Most of the RPL6 structure is accessible from the outside. (**B**, **C**) Superimposition of replica 3 structure of the CacyBP/SIP-RPL6 complex (from Fig. 3D) on the C-terminal domain of RPL6 in the ribosome. In (**B**), the conformations of the C-terminal domain long flexible loop of RPL6 (pink, from the CacyBP/SIP-RPL6 complex, and cyan, from the crystal structure of ribosome) are indicated by arrows. The C-terminal domain of CacyBP/SIP is not visible since it overlaps with other ribosomal proteins. In (**C**), the C-terminal domain of CacyBP/SIP was taken out of the ribosome keeping the interactions of its middle domain with the long loop of RPL6 C-terminal domain intact. The CacyBP/SIP-RPL6 complex is shown in the same colors as in Fig. 3

does not interact with other ribosomal components. Since the N-terminal domain of CacyBP/SIP is located outside the prospective CacyBP/SIP-RPL6 complex, the dimerization of CacyBP/SIP does not influence the binding.

Presence of the CacyBP/SIP-RPL6 complexes in the cell including the ribosomal fraction

Having confirmed the possibility of binding between the two proteins in silico, we applied the PLA assay to check if the CacyBP/SIP-RPL6 interaction occurs in the cell. The obtained results show that CacyBP/SIP forms complexes with RPL6 (Fig. 5). In the negative control, when the ligase was omitted, no or barely detectable signals are visible. This result indicates that interaction between CacyBP/SIP and RPL6 takes place in the cell.

RPL6 is a component of the 60 S large ribosomal subunit (Anger et al. 2013). CacyBP/SIP was previously shown to interact with NPM1, which is involved in functions related to ribosomes (Okuwaki et al. 2021; Jr Maggi et al. 2008). Thus, we checked the presence of CacyBP/SIP in the ribosomal fractions. For that, we performed sucrose gradient centrifugation and obtained a typical pattern of polysome fractionation with peaks corresponding to 40S, 60S and 80S ribosomal fractions from top to bottom (Fig. 6A). The results of Western blot analysis of fractions collected after gradient centrifugation showed that CacyBP/SIP was present together with RPL6 in fractions containing the 60S large ribosomal subunit (fractions 13–14) (Fig. 6B). This indicates that CacyBP/SIP may be involved in ribosomal function and regulation of translation.

Potential impact of CacyBP/SIP on protein synthesis and on the ER structure/network

Having confirmed the presence of CacyBP/SIP on the 60S large ribosomal subunit (Fig. 6), we decided to investigate its impact on protein synthesis. For that, *via* cell transfection with plasmids encoding target-specific or non-target control shRNA and subsequent selection of cell clones, we obtained stable NB2a cell lines with endogenous or diminished CacyBP/SIP level, referred to as control (Ctrl) and CacyBP/SIP-KD, respectively. The efficiency of CacyBP/SIP silencing at the mRNA and protein level was in the range of 50% (Fig. 7A and B). To these cells we applied OPP (O-propargyl-puromycin), a puromycin analogue that efficiently incorporates into newly synthesized polypeptides, which are then labelled with a fluorescent Alexa 488 dye *via* click-chemistry. The resulting fluorescent product visualized under the confocal microscope can be regarded

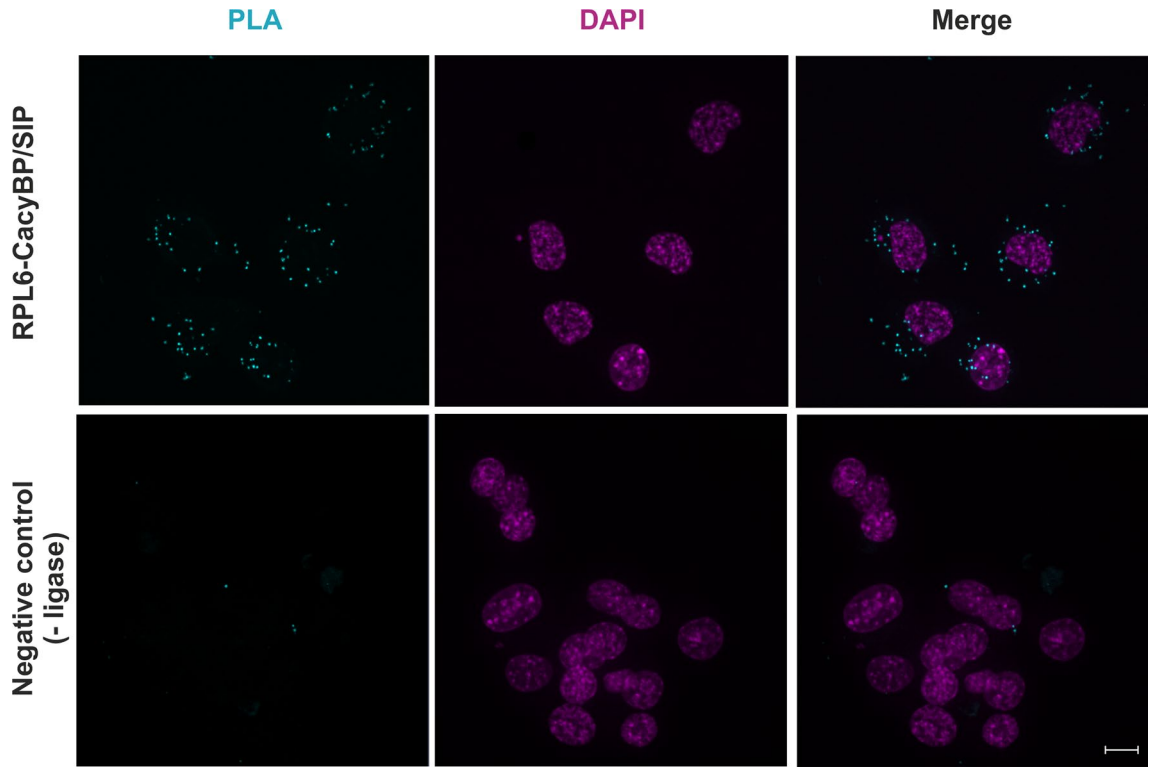

Fig. 5 CacyBP/SIP-RPL6 complexes in NB2a cells detected by proximity ligation assay (PLA). Cyan PLA signals represent CacyBP/SIP-RPL6 complexes while nuclei are marked in purple. Scale bar is 10 µm

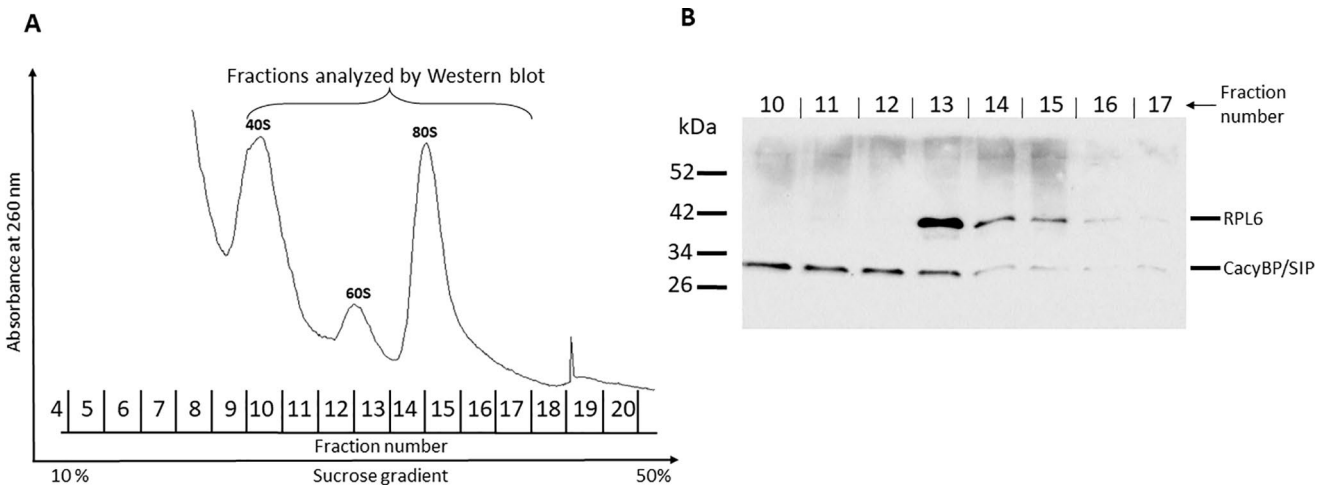

Fig. 6 Presence of CacyBP/SIP and RPL6 proteins on the 60S large ribosomal subunit. (**A**) Absorbance (A_{260}) profile of fractions collected after sucrose gradient (10–50%) ultracentrifugation of the lysate from NB2a cells. (**B**) Western blot analysis of particular fractions obtained after sucrose gradient ultracentrifugation / polysome profiling (see Materials and Methods section for details)

as a signal of protein synthesis, illustrating the intensity and localization of translation in the cytoplasm. In control cells the pattern of enhanced OPP staining, mostly in the perinuclear area was reminiscent of the rough ER localization (Fig. 7C; bright green areas indicated by white arrows; see also Supporting information file and Fig. S3 for better contrast). In cells with diminished CacyBP/SIP level, the fluorescence signal originating from OPP-Alexa was dispersed in the cytoplasm. Analysis of the confocal images has shown that after 30 min incubation with 20 µM OPP the number of cells with enhanced OPP staining was about 3 times lower in CacyBP/SIP-KD cell line than in the control one (Fig. 7D). The bright OPP signal visible in the nuclei/nucleoli may originate from the so-called amyloid bodies, that it sites of local nuclear protein synthesis (LNPS) (Theodoridis et al. 2021).

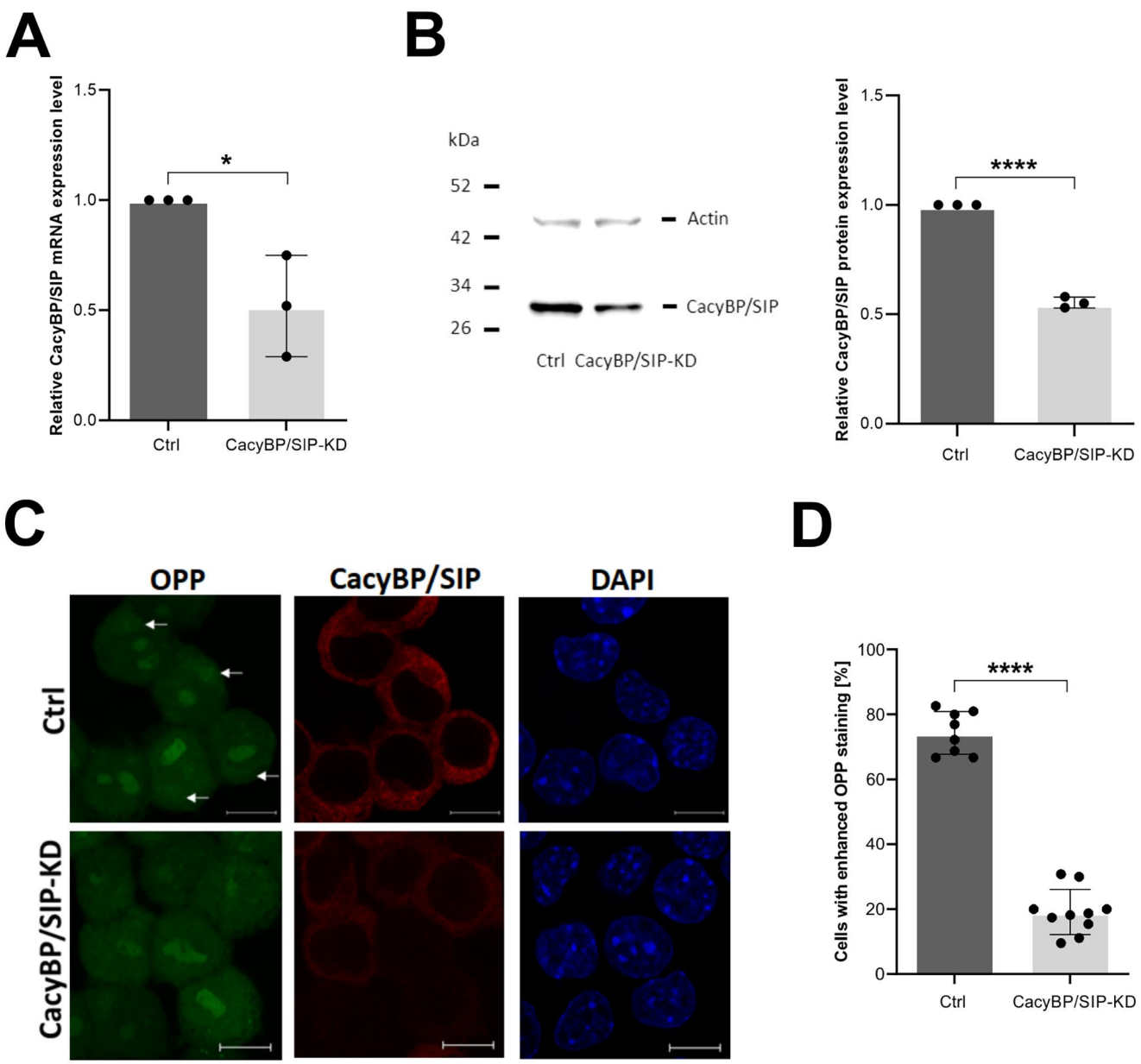

Fig. 7 CacyBP/SIP mRNA (**A**) and CacyBP/SIP protein level (**B**) in stably transfected NB2a cell lines. Representative immunoblot (**B**, left panel) and densitometric analysis (**B**, right panel). Ctrl – cells transfected with plasmid containing scramble shRNA; CacyBP/SIP-KD – cells transfected with shRNA-CacyBP/SIP plasmid. Bars indicate mean ± SD. Student's *t*-test was used. The individual data points (dots) are shown; $*p < 0.05$. Influence of CacyBP/SIP knock-down on protein synthesis in NB2a cells (**C** and **D**). (**C**) Confocal images of control NB2a cells (Ctrl; upper panel) and NB2a with diminished CacyBP/SIP level (CacyBP/SIP-KD; lower panel). OPP (green), CacyBP/SIP (red) and DAPI (blue). The white arrows show enhanced OPP staining within the cytoplasm. Scale bar is 10 µm. (**D**) Statistical analysis of results presented in (**C**). Data are presented as mean ± SD and Student's *t*-test was used. The individual data points (dots) are shown; $****p \leq 0.0001$

Since OPP staining suggested that higher cellular CacyBP/SIP level coincided with enhanced protein synthesis in NB2a cells, we decided to check whether CacyBP/SIP deficiency might somehow affect the ER architecture/network. To this end we performed staining of ER using the ER-Tracker dye. As can be seen in Fig. S4A, the intensity of ER staining differed between control and CacyBP/SIP-KD cells. Statistical analysis showd that the fluorescence intensity of ER staining was about 60% lower in CacyBP/SIP-KD cells than in control ones (Fig. S4B). We decided to further explore this issue taking advantage of the fact that expression of heat shock proteins (Hsps) is highly induced in cells subjected to stress conditions and, thus, their level may be indicative of the efficiency of protein synthesis. For that,

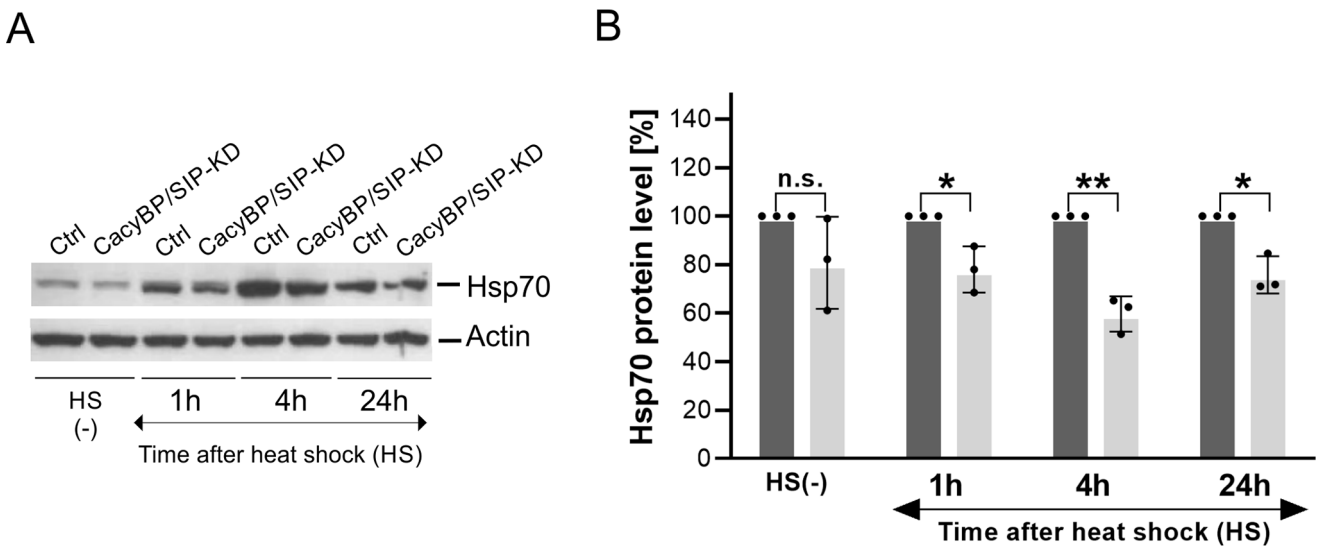

Fig. 8 Effect of CacyBP/SIP knock-down on the level of Hsp70 after heat shock. (**A**) Representative Western blot showing Hsp70 level in control (Ctrl) and CacyBP/SIP-KD NB2a cells, not exposed or exposed to heat shock (HS) and collected after indicated time points. (**B**) Densitometric analysis of the Western blot results. Black and grey bars represent NB2a cells transfected with shRNA-control plasmid (Ctrl) or with shRNA-CacyBP/SIP plasmid (CacyBP/SIP-KD), respectively. Bars indicate mean ± SD. Student's *t*-test was used. The individual data points (dots) are shown; n.s. – non-significant, $*p \leq 0.05$, $**p \leq 0.01$

we performed an experiment in which CacyBP/SIP-KD and control NB2a cells were subjected to heat shock and then the cell lysates were examined by Western blot to estimate the rise in the level of Hsp70, the most highly induced heat shock protein. We found that Hsp70 level increased in both control and CacyBP/SIP-KD cell lines after heat shock, but this increase was significantly higher in the control cells compared to CacyBP/SIP-KD cells (Fig. 8). Although the above results should be confirmed by more thorough analyses, it cannot be excluded that CacyBP/SIP, possibly through interaction with RPL6 and/or other RPs, may be involved in regulation of ribosomal function.

Discussion

CacyBP/SIP is a protein expressed in various mammalian tissues and cells, and is localized mainly in the cytoplasm. It interacts with several target proteins and is involved in multiple cellular processes (Topolska-Woś et al. 2016). Previously, we have shown that CacyBP/SIP is present in the nucleus and interacts with a nucleolar protein NPM1 (Rosińska and Filipek 2018). In this work we investigated the potential involvement of CacyBP/SIP in ribosome assembly and/or function. At first, we performed mass spectrometry analysis to identify CacyBP/SIP targets functionally linked with ribosomes. Indeed, we found that several ribosomal proteins (RPs), among them RPL6 - a component of the 60S large ribosomal subunit, could be potential CacyBP/SIP targets. As assessed by co-immunoprecipitation, PLA and ELISA, RPL6 interacted with CacyBP/SIP both in vitro, when recombinant proteins were used, and in the cell.

A direct character of the interaction between these two proteins, which could be inferred from the ELISA results, was further supported by in silico protein-protein docking studies. The docking studies, based on the isolated domains of both proteins, revealed that all domains of CacyBP/SIP can form favorable interactions, mostly electrostatic but also hydrophobic, with the C-terminal domain of RPL6. The interactions between C-terminal domains of both proteins were the strongest and the middle domain of CacyBP/SIP was ranked the second. Since the contact area of the middle domain of CacyBP/SIP involved the ends of the long flexible loop of RPL6, which was removed before the docking procedure, restoration of this loop was not possible. Therefore, the most probable structure of the complex involved a contact between the C-terminal domains of both proteins and this structure was selected for molecular dynamics (MD) simulations, which were conducted in three replicas. During the simulations, the other two domains of CacyBP/SIP also interacted with RPL6 but their interactions were weak, except for the middle domain of CacyBP/SIP in replica 3. In this case, the middle domain of CacyBP/SIP formed a rather extensive contact with a long loop of the C-terminal domain of RPL6.

Since RPL6 is located on the top of the ribosome 60S subunit, large parts of this protein are accessible from the outside. This is especially true for the long flexible loop from the C-terminal domain, which is thus accessible for binding to the middle domain of CacyBP/SIP. To test this

possibility, we superimposed the complex obtained from replica 3 simulation, onto the ribosome. This superimposition was based on the overlapping of the C-terminal domains of RPL6. In the resulting structure, the C-terminal domain of CacyBP/SIP was found inside the ribosome, however, the other two domains of this protein did not have contacts with the ribosomal structure. To check if it is possible to extract the C-terminal domain of CacyBP/SIP from the ribosome, we moved the isolated C-terminal domain of CacyBP/SIP outside and connected it again with the linker. Since the linker between the C-terminal and middle domains is long and flexible, such procedure resulted in a correct structure of CacyBP/SIP. Our findings argue for the possibility that CacyBP/SIP is able to bind not only to free RPL6 but also when it is incorporated in the ribosome. In the former case the C-terminal domain of CacyBP/SIP is involved, but in the latter one the middle domain is essential. The final structure of the complex suggests that the long loop of the RPL6 C-terminal domain is accessible for interactions with other proteins, including CacyBP/SIP, which finally can influence the ribosome function.

Ribosomes consist of a small 40S subunit and a large 60S subunit. Together, both subunits are composed of 4 RNA species and approximately 80 structurally distinct ribosomal proteins (RPs). Numerous other proteins are engaged in the assembly and maturation of ribosomal subunits in the nucleolus (Bohnsack and Bohnsack 2019). Both CacyBP/SIP targets, NPM1 and RPL6, are important players in ribosome biogenesis and function. NPM1 and other ribosome-assembly proteins take part in the late maturation step of the pre-60S ribosomal subunit (Okuwaki et al. 2021). RPL6 is a component of a mature large ribosomal subunit (Anger et al. 2013). It also plays a role in regulating the DNA damage response (DDR) (Yang et al. 2019) and nucleolar stress-induced p53 activation (Bai et al. 2014). Thus, we presumed that CacyBP/SIP, *via* interaction with RPL6 and/or NPM1, may be involved in some stages of the process of protein synthesis. To examine this, we treated cells with OPP, which incorporates into newly synthesized polypeptides and can thus serve as an indicator of the intensity and localization of translation. We found that the number of cells with high fluorescence intensity, indicative of the ongoing translation, was about 3 times lower in the NB2a cell line with diminished CacyBP/SIP level than in the control cell line. Moreover, in control cells the enhanced OPP staining formed a pattern reminiscent of the localization of rough ER. However, in cells with diminished CacyBP/SIP, this pattern was absent, and the signal was dispersed in the cytoplasm. In addition, we showed a smaller increase in the level of stress-inducible Hsp70 protein in CacyBP/SIP-KD NB2a cells exposed to heat shock.

Since the rough ER is a significant site of protein synthesis in all eukaryotic cells, we analyzed the effect of CacyBP/SIP on the ER architecture/network. ER is a continuous membrane system, consisting of flattened cisternae and elongated tubules, which extend from the nuclear envelope (NE) to the vicinity of the plasma membrane and contact other cellular organelles, e.g. mitochondria, the Golgi apparatus, lysosomes and endosomes (Schwarz and Blower 2016). The surface of the rough ER is covered with protein-producing ribosomes. Once the protein has been synthesized, membrane-bound transport vesicles relocate it to the Golgi apparatus. Interestingly, we found that in neuroblastoma NB2a cells with diminished CacyBP/SIP level the staining intensity of ER, detected with the ER-Tracker dye, was about 60% lower than in control ones. This interesting finding can be interpreted in several ways. First, the structure, volume and dynamics of ER largely depend on the microtubule network (Waterman-Strorer and Salmon, 1998) and the actin cytoskeleton (Pain et al. 2023). CacyBP/SIP has been shown to interact with both tubulin and actin (Schneider et al. 2010). Consequently, CacyBP/SIP deficiency in a cell may disturb or rearrange the microfilament and microtubule organization, which in turn may disturb the ER network. It is also known that ER is a very dynamic structure, and the ER mass adapts to the metabolic needs of a cell (Sanz-Martinez and Stolz 2022). In this regard, CacyBP/SIP deficiency has been often correlated with diminished cell proliferation and, hence, with lower energetic cost, that can be reflected in the range of the ER network (Chen et al. 2011). Nonetheless, the effect of altered CacyBP/SIP level on the ER architecture and functionality requires further studies.

Overall, our results demonstrated a direct interaction between CacyBP/SIP and the ribosomal protein RPL6 and localized the binding to the C-terminal domains of both proteins with a potential involvement of the middle domain of CacyBP/SIP, especially when the binding occurs in the ribosome. Furthermore, results obtained using CacyBP/SIP-KD cells allow us to speculate that CacyBP/SIP either directly, through interaction with RPL6 and/or other RPs, or indirectly, by way of its influence on the cytoskeleton and the ER network, may affect ribosome function including protein synthesis. However, at present, it is difficult to envisage the exact mechanism of CacyBP/SIP action. It is known that the protein is a component of various protein complexes, and its major role is to stabilize the association of their respective constituents. Thus, one can presume that the contribution of CacyBP/SIP to the formation of the ribosome complex may rely on its scaffolding properties. Further studies are still needed to resolve this issue.

Supplementary Information The online version contains supplementary material available at https://doi.org/10.1007/s00726-025-03464-3.

Acknowledgements This work was supported by grant 2018/29/B/NZ4/01384 to A.F. from the National Science Centre and by statutory funds from the Nencki Institute of Experimental Biology of the Polish Academy of Sciences. Fluorescent imaging was performed at the Laboratory of Imaging Tissue Structure and Function, which serves as an imaging core facility at the Nencki Institute of Experimental Biology and is part of the infrastructure of the Polish Euro-BioImaging Node.

Author contributions A. Filipek, A. Starosta, E. Kilańczyk, P. Bieganowski and S. Filipek conceived and designed the research; E. Jurewicz, M. Maksymowicz-Trivedi, O. Saberi-Khomami, O. Iwańska, A. Jarmuła, performed the research and acquired the data; A. Filipek, A. Starosta S. Filipek, E. Jurewicz, M. Maksymowicz-Trivedi and W. Leśniak analyzed and interpreted the data. All authors were involved in drafting and revising the manuscript.

Data availability The mass spectrometry proteomics data have been deposited to the ProteomeXchange Consortium via the PRIDE (Perez-Riverol Y et al., 2025) partner repository with the dataset identifier PXD064560 and 10.6019/PXD064560". Other data are provided within the manuscript or supplementary information files.

Declarations

Competing interests The authors declare no competing interests.

References

Anger AM, Armache JP, Berninghausen O, Habeck M, Subklewe M, Wilson DN, Beckmann R (2013) Structures of the human and Drosophila 80S ribosome. Nature 497:80–85. https://doi.org/10.1038/nature12104

Bai D, Zhang J, Xiao W, Zheng X (2014) Regulation of the HDM2-p53 pathway by ribosomal protein L6 in response to ribosomal stress. Nucleic Acids Res 42:1799–1811. https://doi.org/10.1093/nar/gkt971

Berendsen HJC, Postma JPM, DiNola A, Haak JR (1984) Molecular dynamics with coupling to an external bath. J Chem Phys 81:3684–3690. https://doi.org/10.1063/1.448118

Bohnsack KE, Bohnsack MT (2019) Uncovering the assembly pathway of human ribosomes and its emerging links to disease. EMBO J 38:e100278. https://doi.org/10.15252/embj.2018100278

Case DA, Aktulga HM, Belfon K, Ben-Shalom I, Berryman JT, Brozell SR, Cerutti DS, Cheatham TE III, Cisneros GA, Cruzeiro VWD, Darden TA, Duke R, Giambasu G, Gilson MK, Gohlke H, Goetz AW, Harris R, Izadi S, Izmailov SA, Kasavajhala K, Kaymak MC, King E, Kovalenko A, Kurtzman T, Lee T, LeGrand S, Li P, Lin C, Liu J, Luchko T, Luo R, Machado M, Man VH, Manathunga M, Merz K, Miao Y, Mikhailovskii M, Monard G, Nguyen H, O'Hearn K, Onufriev A, Pan F, Pantano S, Qi R, Rahnamoun A, Roe DR, Roitberg A, Sagui C, Schott-Verdugo S, Shayan A, Shen J, Simmerling CL, Skrynnikov N, Smith J, Swails JM, Walker RC, Wang J, Wei H, Wolf RM, Wu X, Xiong Y, Xue Y, York DM, Zao S, Kollman PA (2022) AMBER, University of California, San Francisco

Chen X, Mo P, Li X, Zheng P, Zhao L, Xue Z, Ren G, Han G, Wang X, Fan D (2011) CacyBP/SIP protein promotes proliferation and G1/S transition of human pancreatic cancer cells. Mol Carcinog 50:804–810. https://doi.org/10.1002/mc.20737

Desta IT, Porter KA, Xia B, Kozakov D, Vajda S (2020) Performance and its limits in rigid body Protein-Protein Docking. Structure 28:1071–1081e3. https://doi.org/10.1016/j.str.2020.06.006

Dimitrova YN, Li J, Lee YT, Rios-Esteves J, Friedman DB, Choi HJ, Weis WI, Wang CY, Chazin WJ (2010) Direct ubiquitination of beta-catenin by Siah-1 and regulation by the exchange factor TBL1. J Biol Chem 285:13507–13516. https://doi.org/10.1074/jbc.M109.049411

Filipek A, Kuźnicki J (1998) Molecular cloning and expression of a mouse brain cDNA encoding a novel protein target of Calcyclin. J Neurochem 70:1793–1798. https://doi.org/10.1046/j.1471-4159.1998.70051793.x

Filipek A, Leśniak W (2018) Current view on cellular function of S100A6 and its ligands, CacyBP/SIP and Sgt1. Postepy Biochem 64:242–252. https://doi.org/10.18388/pb.2018_136

Filipek A, Wojda U (1996) p30, a novel protein target of mouse Calcyclin (S100A6). Biochem J 320:585–587. https://doi.org/10.1042/bj3200585

Filipek A, Jastrzebska B, Nowotny M, Kuznicki J (2002) CacyBP/SIP, a Calcyclin and Siah-1-interacting protein, binds EF-hand proteins of the S100 family. J Biol Chem 277:28848–288852. https://doi.org/10.1074/jbc.M203602200

Jarmuła A, Wilk P, Maj P, Ludwiczak J, Dowierciał A, Banaszak K, Rypniewski W, Cieśla J, Dąbrowska M, Frączyk T, Bronowska AK, Jakowiecki J, Filipek S, Rode W (2017) Crystal structures of nematode (parasitic T. spiralis and free living C. elegans), compared to mammalian, thymidylate synthases (TS). Molecular Docking and molecular dynamics simulations in search for nematode-specific inhibitors of TS. J Mol Graph Model 77:33–50. https://doi.org/10.1016/j.jmgm.2017.08.008

Jastrzebska B, Filipek A, Nowicka D, Kaczmarek L, Kuznicki J (2000) Calcyclin (S100A6) binding protein (CacyBP) is highly expressed in brain neurons. J Histochem Cytochem 48:1195–1202. https://doi.org/10.1177/002215540004800903

Jr Maggi LB, Kuchenruether M, Dadey DY, Schwope RM, Grisendi S, Townsend RR, Pandolfi PP, Weber JD (2008) Nucleophosmin serves as a rate-limiting nuclear export chaperone for the mammalian ribosome. Mol Cell Biol 28:7050–7065. https://doi.org/10.1128/MCB.01548-07

Jurewicz E, Ostrowska Z, Jozwiak J, Redowicz MJ, Lesniak W, Moraczewska J, Filipek A (2013) CacyBP/SIP as a novel modulator of the thin filament. Biochim Biophys Acta 1833:761–766. https://doi.org/10.1016/j.bbamcr.2012.12.010

Kilanczyk E, Filipek S, Jastrzebska B, Filipek A (2009) CacyBP/SIP binds ERK1/2 and affects transcriptional activity of Elk-1. Biochem Biophys Res Commun 380:54–59. https://doi.org/10.1016/j.bbrc.2009.01.026

Krieger E, Vriend G (2015) New ways to boost molecular dynamics simulations. J Comput Chem 36:996–1007. https://doi.org/10.1002/jcc.2389

Krieger E, Koraimann G, Vriend G (2002) Increasing the precision of comparative models with YASARA NOVA–a self-parameterizing

force field. Proteins 47:393–402. https://doi.org/10.1002/prot.10104

Laemmli UK (1970) Cleavage of structural proteins during the assembly of the head of bacteriophage T4. Nature 227:680–685. https://doi.org/10.1038/227680a0

Li MZ, Elledge SJ (2012) SLIC: a method for sequence- and ligation-independent cloning. Methods Mol Biol 852:51–59. https://doi.org/10.1007/978-1-61779-564-0_5

Li H, Huo Y, He X, Yao L, Zhang H, Cui Y, Xiao H, Xie W, Zhang D, Wang Y, Zhang S, Tu H, Cheng Y, Guo Y, Cao X, Zhu Y, Jiang T, Guo X, Qin Y, Sha J (2022) A male germ-cell-specific ribosome controls male fertility. Nature 612:725–731. https://doi.org/10.1038/s41586-022-05508-0

Liu J, Stevens J, Rote CA, Yost HJ, Hu Y, Neufeld KL, White RL, Matsunami N (2001) Siah-1 mediates a novel beta-catenin degradation pathway linking p53 to the adenomatous polyposis coli protein. Mol Cell 7:927–936. https://doi.org/10.1016/s1097-2765(01)00241-6

Matsuzawa SI, Reed JC (2001) Siah-1, SIP, and Ebi collaborate in a novel pathway for beta-catenin degradation linked to p53 responses. Mol Cell 7:915–926. https://doi.org/10.1016/s1097-2765(01)00242-8

Mehta S, Bernt M, Chambers M, Fahrner M, Föll MC, Gruening B, Horro C, Johnson JE, Loux V, Rajczewski AT, Schilling O, Vandenbrouck Y, Gustafsson OJR, Thang WCM, Hyde C, Price G, Jagtap PD, Griffin TJ (2023) A galaxy of informatics resources for MS-based proteomics. Expert Rev Proteom 20:251–266. https://doi.org/10.1080/14789450.2023.2265062

Ning X, Chen Y, Wang X, Li Q, Sun S (2016) The potential role of CacyBP/SIP in tumorigenesis. Tumour Biol 37:10785–10791. https://doi.org/10.1007/s13277-016-4871-y

Okuwaki M, Saito S, Hirawake-Mogi H, Nagata K (2021) The interaction between nucleophosmin/NPM1 and the large ribosomal subunit precursors contribute to maintaining the nucleolar structure. Biochim Biophys Acta 1868:118879. https://doi.org/10.1016/j.bbamcr.2020.118879

Pain C, Tolmie F, Wojcik S, Wang P, Kriechbaumer V (2023) intER-ACTINg: the structure and dynamics of ER and actin are interlinked. J Microsc 291:105–118. https://doi.org/10.1111/jmi.13139

Perez-Riverol Y, Bandla C, Kundu DJ, Kamatchinathan S, Bai J, Hewapathirana S, John NS, Prakash A, Walzer M, Wang S, Vizcaíno JA (2025) The PRIDE database at 20 years: 2025 update. Nucleic Acids Res 53(D1):D543–D553. https://doi.org/10.1093/nar/gkae1011

Rosińska S, Filipek A (2018) Interaction of CacyBP/SIP with NPM1 and its influence on NPM1 localization and function in oxidative stress. J Cell Physiol 233:8826–8838. https://doi.org/10.1002/jcp.26797

Sanz-Martinez P, Stolz A (2022) Mechanisms and physiological functions of ER-phagy. Curr Opin Physiol 30:100613. https://doi.org/10.1016/j.cophys.2022.100613

Schneider G, Nieznanski K, Kilanczyk E, Bieganowski P, Kuznicki J, Filipek A (2007) CacyBP/SIP interacts with tubulin in neuroblastoma NB2a cells and induces formation of globular tubulin assemblies. Biochim Biophys Acta 1773:1628–1636. https://doi.org/10.1016/j.bbamcr.2007.07.013

Schneider G, Nieznanski K, Jozwiak J, Slomnicki LP, Redowicz MJ, Filipek A (2010) Tubulin binding protein, cacybp/sip, induces actin polymerization and May link actin and tubulin cytoskeletons. Biochim Biophys Acta 1803:1308–1317. https://doi.org/10.1016/j.bbamcr.2010.07.003

Schwarz DS, Blower MD (2016) The Endoplasmic reticulum: structure, function and response to cellular signaling. Cell Mol Life Sci 73:79–94. https://doi.org/10.1007/s00018-015-2052-6

Theodoridis PR, Bokros M, Marijan D, Balukoff NC, Wang D, Kirk CC, Budine TD, Goldsmith HD, Wang M, Audas TE, Lee S (2021) Local translation in nuclear condensate amyloid bodies. Proc Natl Acad Sci U S A 118:e2014457118. https://doi.org/10.1073/pnas.2014457118

Topolska-Woś AM, Shell SM, Kilańczyk E, Szczepanowski RH, Chazin WJ, Filipek A (2015) Dimerization and phosphatase activity of calcyclin-binding protein/Siah-1 interacting protein: the influence of oxidative stress. FASEB J 29:1711–1724. https://doi.org/10.1096/fj.14-264770

Topolska-Woś AM, Chazin WJ, Filipek A (2016) CacyBP/SIP–Structure and variety of functions. Biochim Biophys Acta 1860:79–85. https://doi.org/10.1016/j.bbagen.2015.10.012

Varadi M, Anyango S, Deshpande M, Nair S, Natassia C, Yordanova G, Yuan D, Stroe O, Wood G, Laydon A, Žídek A, Green T, Tunyasuvunakool K, Petersen S, Jumper J, Clancy E, Green R, Vora A, Lutfi M, Figurnov M, Cowie A, Hobbs N, Kohli P, Kleywegt G, Birney E, Hassabis D, Velankar S (2022) AlphaFold protein structure database: massively expanding the structural coverage of protein-sequence space with high-accuracy models. Nucleic Acids Res 50:D439–D444. https://doi.org/10.1093/nar/gkab1061

Varadi M, Bertoni D, Magana P, Paramval U, Pidruchna I, Radhakrishnan M, Tsenkov M, Nair S, Mirdita M, Yeo J, Kovalevskiy O, Tunyasuvunakool K, Laydon A, Žídek A, Tomlinson H, Hariharan D, Abrahamson J, Green T, Jumper J, Birney E, Steinegger M, Hassabis D, Velankar S (2024) AlphaFold protein structure database in 2024: providing structure coverage for over 214 million protein sequences. Nucleic Acids Res 52:D368–D375. https://doi.org/10.1093/nar/gkad1011

Waterman-Storer CM, Salmon ED (1998) Endoplasmic reticulum membrane tubules are distributed by microtubules in living cells using three distinct mechanisms. Curr Biol J 8:798–806. https://doi.org/10.1016/s0960-9822(98)70321-5

Yang C, Zang W, Ji Y, Li T, Yang Y, Zheng X (2019) Ribosomal protein L6 (RPL6) is recruited to DNA damage sites in a poly(ADP-ribose) polymerase-dependent manner and regulates the DNA damage response. J Biol Chem 294:2827–2838. https://doi.org/10.1074/jbc.RA118.007009

Zhai H, Shi Y, Jin H, Li Y, Lu Y, Chen X, Wang J, Ding L, Wang X, Fan D (2008) Expression of calcyclin-binding protein/Siah-1 interacting protein in normal and malignant human tissues: an immunohistochemical survey. J Histochem Cytochem 56:765–772. https://doi.org/10.1369/jhc.2008.950519